

Bounding the Population Size of IPOP-CMA-ES on the Noiseless BBOB Testbed

Tianjun Liao
IRIDIA, CoDE, Université Libre de Bruxelles
(ULB), Brussels, Belgium
tliao@ulb.ac.be

Thomas Stützle
IRIDIA, CoDE, Université Libre de Bruxelles
(ULB), Brussels, Belgium
stuetzle@ulb.ac.be

ABSTRACT

A variant of CMA-ES that uses occasional restarts coupled with an increasing population size, which is called IPOP-CMA-ES, has shown to be a top performing algorithm on the BBOB benchmark set. In this paper, we test a mechanism that bounds the maximum size that the population may reach in IPOP-CMA-ES, and we experimentally explore the impact of a maximum population size on the BBOB benchmark set. In the proposed bounding mechanism, we use a maximum population size of $10 \times D^2$, where D is problem dimension. Once the maximum population size is reached or surpassed, the population size is reset to its default starting value λ , which is defined by the $\lambda = 4 + \lfloor 3 \ln(D) \rfloor$. Our experimental results show that our scheme for the population-size update can lead to improved performances on separable and weakly structured multi-modal functions.

Categories and Subject Descriptors

G.1.6 [Numerical Analysis]: Optimization—*global optimization, unconstrained optimization*; F.2.1 [Analysis of Algorithms and Problem Complexity]: Numerical Algorithms and Problems

General Terms

Algorithms

Keywords

Benchmarking, Black-box optimization

1. INTRODUCTION

IPOP-CMA-ES [1] is a variant of CMA-ES [11, 10] that uses occasional restarts, which are triggered when the search process is deemed to stagnate, combined with an increasing population size. IPOP-CMA-ES and several of its variants [12, 3, 4, 2] have shown very good results on the BBOB

benchmark. In this paper, we base our analysis on IPOP-CMA-ES using its default parameter settings. In particular, the initial population size in IPOP-CMA-ES is set to $\lambda = 4 + \lfloor 3 \ln(D) \rfloor$, where D is dimension of the problem being tackled. At each restart, IPOP-CMA-ES increases the population size by a factor of two. This setting leads to an exponential increase of the population size in IPOP-CMA-ES in the number of restarts. In particular, on difficult, multi-modal functions many restarts may occur and, thus, very large population sizes may result if IPOP-CMA-ES doesn't find a solution better than the optimal threshold or a possible target value.

In this paper, we use a mechanism to bound the maximum population size that IPOP-CMA-ES may use; in fact, bounding the maximum population size is motivated by the fact that sometimes very large populations may, at least theoretically, decrease the performances [5]. However, occasionally CMA-ES may benefit from large populations [9], which is also the motivation for increasing the population size in IPOP-CMA-ES. Thus, in our bound on the population size, we do not want to be too restrictive. Thus, we set the upper bound of the population size to $10 \times D^2$, which leaves for higher dimensional problems the possibility to reach rather large populations (e.g. 16 000 for $D = 40$). Once this upper bound is reached, we reset the population size to its initial value, given by $\lambda = 4 + \lfloor 3 \ln(D) \rfloor$. Additionally, it gives some additional robustness with respect to the maximum bound on the population size we use. We label the resulting IPOP-CMA-ES variant IP-10DDr. The original IPOP-CMA-ES is labeled IP.

2. EXPERIMENTAL PROCEDURE

We used the C version of IPOP-CMA-ES (last modification date 10/16/10) from Hansen's webpage <http://www.lri.fr/~hansen/cmaesintro.html>. To ensure that the final best solution is inside the bounds, the bound constraints are enforced by clamping each generated solution that violates the bound constraint to the nearest solution on the bounds. The default parameter settings of IPOP-CMA-ES were used. A maximum of $10^6 \times D$ function evaluations was used for the experiments.

3. RESULTS

The results from the experiments that follow the experimental protocol [7] on the benchmark functions given in [6, 8] are presented in Figures 1, 3 and 4 and in Tables 1 and 2. The **expected running time (ERT)**, used in the figures and tables, depends on a given target function value,

Permission to make digital or hard copies of all or part of this work for personal or classroom use is granted without fee provided that copies are not made or distributed for profit or commercial advantage and that copies bear this notice and the full citation on the first page. To copy otherwise, to republish, to post on servers or to redistribute to lists, requires prior specific permission and/or a fee.

GECCO'13 Companion, July 6–10, 2013, Amsterdam, The Netherlands.
Copyright 2013 ACM 978-1-4503-1964-5/13/07 ...\$15.00.

$f_t = f_{\text{opt}} + \Delta f$, and it is computed across all relevant trials as the number of function evaluations executed during each trial while the best function value did not reach f_t , summed over all trials and divided by the number of trials that actually reached f_t [7, 13]. **Statistical significance** is tested with the rank-sum test for a given target Δf_t (10^{-8} as in Figure 1) using, for each trial, either the number of needed function evaluations to reach Δf_t (inverted and multiplied by -1), or, if the target was not reached, the best Δf -value achieved, measured only up to the smallest number of overall function evaluations for any unsuccessful trial under consideration.

In the experiments, we found that IP-10DDr reaches solutions below the optimal threshold of 10^{-8} in various cases where the default version of IPOP-CMA-ES, here labeled IP, could not find such solutions. This was the case for functions f_4 ($D = 3, 5$), f_{21} ($D = 40$), f_{22} ($D = 10$) and f_{24} ($D = 2, 3$). Compared to IP, IP-10DDr uses fewer function evaluations to reach optimal threshold in functions f_3 ($D = 3, 5, 10$), f_{16} ($D = 3$), f_{21} ($D = 2, 3, 5, 10, 20$), f_{22} ($D = 2, 3, 5$), f_{23} ($D = 10, 20$); only in functions f_{19} ($D = 10$) and f_{20} ($D = 5, 10, 20$), IP-10DDr uses slightly more function evaluations to reach optimal threshold than IP.

We next examine the impact of the specific choice on the maximum population size. To do so, we explore another bound mechanism, where the maximum population size is set to a constant value of 500; a population size larger than 500 is then kept to 500. We label the resulting algorithm IP-500. Figure 1 shows that IP-10DDr clearly performs better than IP-500.

To situate the performance of IP-10DDr better with respect to other variants of IPOP-CMA-ES, in Figure 2 we show the comparisons between IP-10DDr and the performance data for the IPOP-CMA-ES variants, CMA_mah [2] and IPOPsaACM [12] in the aforementioned functions $f_3, f_4, f_{16}, f_{19}, f_{20}, f_{21}, f_{22}, f_{23}, f_{24}$. We find that IP-10DDr reaches the optimal threshold in functions f_4 ($D = 5$), f_{19} ($D = 40$), f_{21} ($D = 40$), f_{23} ($D = 20$) and f_{24} ($D = 3$) where both, CMA_mah and IPOPsaACM, cannot reach optimal threshold. In functions f_3 ($D = 3, 5, 10$), f_4 ($D = 2, 3$), f_{16} ($D = 3$), f_{22} ($D = 3, 5$), f_{23} ($D = 3, 5, 10$) IP-10DDr uses fewer function evaluations to reach optimal threshold than CMA_mah and IPOPsaACM.

4. CPU TIMING EXPERIMENT

The IP-10DDr was run on f_3 until at least 30 seconds have passed. These experiment were conducted with Intel Xeon E5410 (2.33 GHz) on Linux (kernel 2.6.9 - 78.0.22). The results were $3.1\text{E}-05$, $1.5\text{E}-05$, $1.2\text{E}-05$, $9.5\text{E}-06$, $1.5\text{E}-05$ and $5.0\text{E}-05$ seconds per function evaluation in dimensions 2, 3, 5, 10, 20, and 40, respectively.

5. CONCLUSIONS

In this paper, we have studied the impact of bounding the population size in IPOP-CMA-ES together with re-initialization of the population size. Obviously, using a maximum population size of $10 \times D^2$ does not worsen results on functions that are easy for IPOP-CMA-ES, that is, on functions where IPOP-CMA-ES within the first trial or very few restarts finds the optimum—in such cases the bounds do not take effect. However, for various difficult, multi-modal functions we observed improved performance of our new IPOP-CMA-ES

variants over the default IPOP-CMA-ES. Hence, these results would encourage us to explore bounds on the maximum population size also for other IPOP-CMA-ES variants such as Bipop-CMA-ES. Finally, one may further explore different settings for the bounds on the maximum population size, which may lead to further improvements in performance.

6. ACKNOWLEDGMENTS

The authors would like to thank the great and hard work of the BBOB team. This work was supported by the Meta-X project funded by the Scientific Research Directorate of the French Community of Belgium. Thomas Stützle acknowledges support from the Belgian F.R.S.-FNRS, of which he is a Research Associate. Tianjun Liao acknowledges a fellowship from the China Scholarship Council.

7. REFERENCES

- [1] A. Auger and N. Hansen. A restart CMA evolution strategy with increasing population size. In *Proceedings of the IEEE Congress on Evolutionary Computation (CEC 2005)*, pages 1769–1776. IEEE Press, 2005.
- [2] D. Brockhoff, A. Auger, and N. Hansen. On the impact of active covariance matrix adaptation in the CMA-ES with mirrored mutations and small initial population size on the noiseless BBOB testbed. In *GECCO 2012 (Companion)*, pages 291–296, 2010.
- [3] D. Brockhoff, A. Auger, and N. Hansen. Comparing mirrored mutations and active covariance matrix adaptation in the IPOP-CMA-ES on the noiseless BBOB testbed. In T. Soule, editor, *GECCO 2012 (Companion)*, pages 297–303. ACM, 2012.
- [4] D. Brockhoff, A. Auger, and N. Hansen. On the impact of a small initial population size in the IPOP active CMA-ES with mirrored mutations on the noiseless BBOB testbed. In T. Soule, editor, *GECCO 2012 (Companion)*, pages 291–296. ACM, 2012.
- [5] T. Chen, K. Tang, G. Chen, and X. Yao. A large population size can be unhelpful in evolutionary algorithms. *Theoretical Computer Science*, 436:54–70, 2012.
- [6] S. Finck, N. Hansen, R. Ros, and A. Auger. Real-parameter black-box optimization benchmarking 2009: Presentation of the noiseless functions. Technical Report 2009/20, Research Center PPE, 2009. Updated February 2010.
- [7] N. Hansen, A. Auger, S. Finck, and R. Ros. Real-parameter black-box optimization benchmarking 2012: Experimental setup. Technical report, INRIA, 2012.
- [8] N. Hansen, S. Finck, R. Ros, and A. Auger. Real-parameter black-box optimization benchmarking 2009: Noiseless functions definitions. Technical Report RR-6829, INRIA, 2009. Updated February 2010.
- [9] N. Hansen and S. Kern. Evaluating the CMA evolution strategy on multimodal test functions. In *Parallel Problem Solving from Nature – PPSN VIII*, volume 3242 of *Lecture Notes in Computer Science*, pages 282–291. Springer, Heidelberg, Germany, 2004.
- [10] N. Hansen, S. Muller, and P. Koumoutsakos. Reducing the time complexity of the derandomized evolution

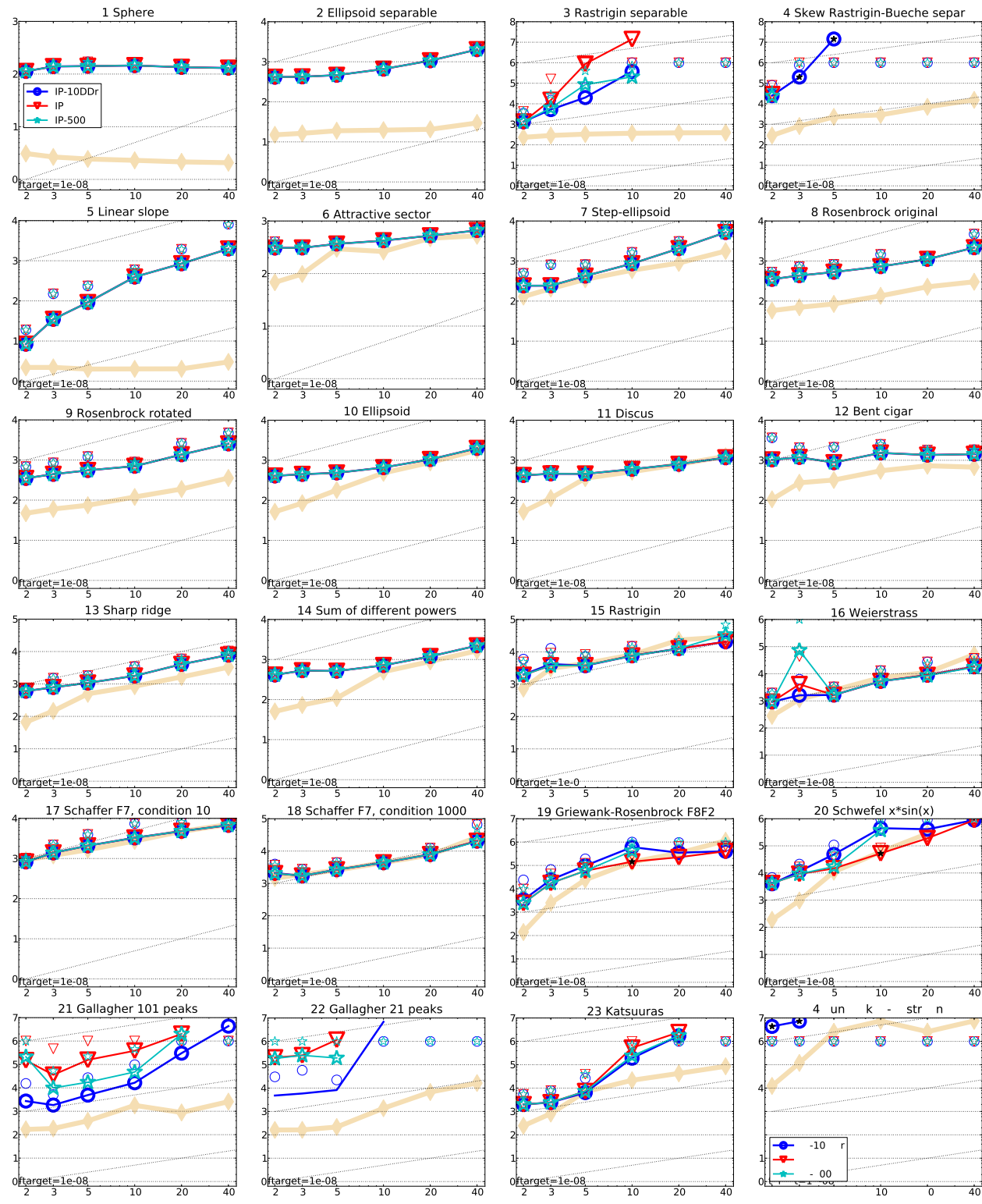


Figure 1: Expected running time (ERT in number of f -evaluations) divided by dimension for target function value 10^{-8} as \log_{10} values versus dimension. Different symbols correspond to different algorithms given in the legend of f_1 and f_{24} . Light symbols give the maximum number of function evaluations from the longest trial divided by dimension. Horizontal lines give linear scaling, slanted dotted lines give quadratic scaling. Black stars indicate statistically better result compared to all other algorithms with $p < 0.01$ and Bonferroni correction number of dimensions (six). Legend: \circ :IP-10DDr, ∇ :IP, \star :IP-500

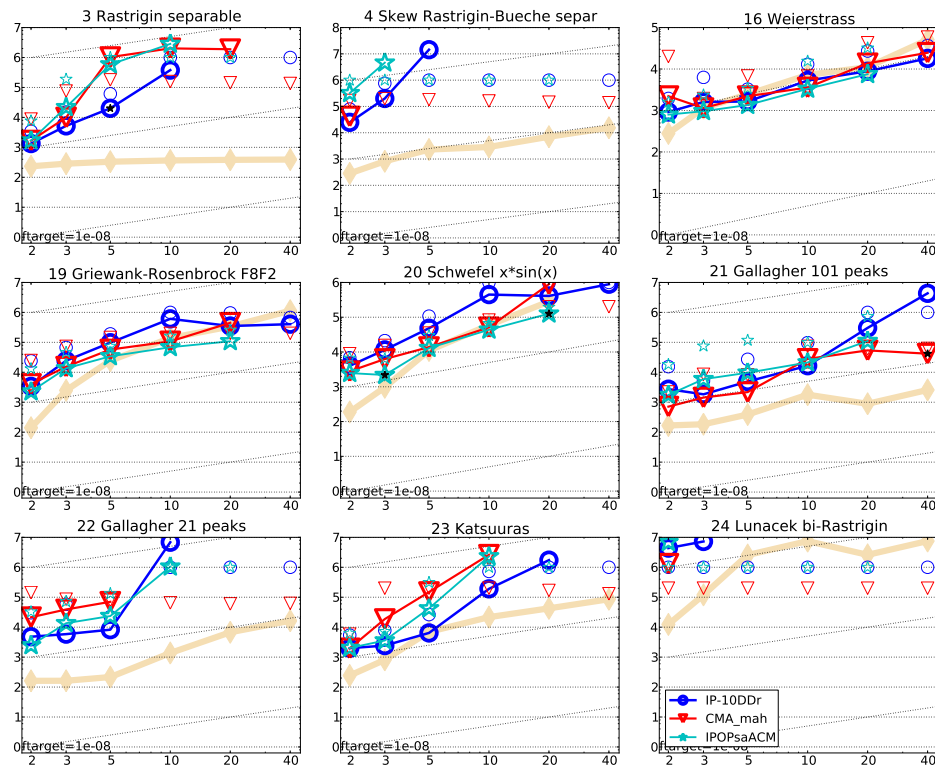


Figure 2: Comparing IP-10DDr to CMA_mah and IPOPsaACM. CMA_mah is the active covariance matrix adaptation version of IPOP-CMA-ES with mirrored mutation and a small initial population size. CMA_sa is self-adaptive surrogate-assisted version of IPOP-CMA-ES. Expected running time (ERT) divided by dimension for target function value 10^{-8} as \log_{10} values. Different symbols correspond to different algorithms given in legend of f_{24} . Light symbols give the maximum number of function evaluations from all trials divided by the dimension. Horizontal lines give linear scaling, the slanted dotted lines give quadratic scaling.

strategy with covariance matrix adaptation (CMA-ES). *Evolutionary Computation*, 11(1):1–18, 2003.

- [11] N. Hansen and A. Ostermeier. Completely derandomized self-adaptation in evolution strategies. *Evolutionary Computation*, 9(2):159–195, 2001.
- [12] I. Loshchilov, M. Schoenauer, and M. Sebag. Black-box optimization benchmarking of IPOP-SaACM-ES and Bipop-SaACM-ES on the BBOB-2012 noiseless testbed.

In T. Soule, editor, *GECCO 2012 (Companion)*, pages 175–182. ACM, 2012.

- [13] K. Price. Differential evolution vs. the functions of the second ICEO. In *Proceedings of the IEEE International Congress on Evolutionary Computation*, pages 153–157, 1997.

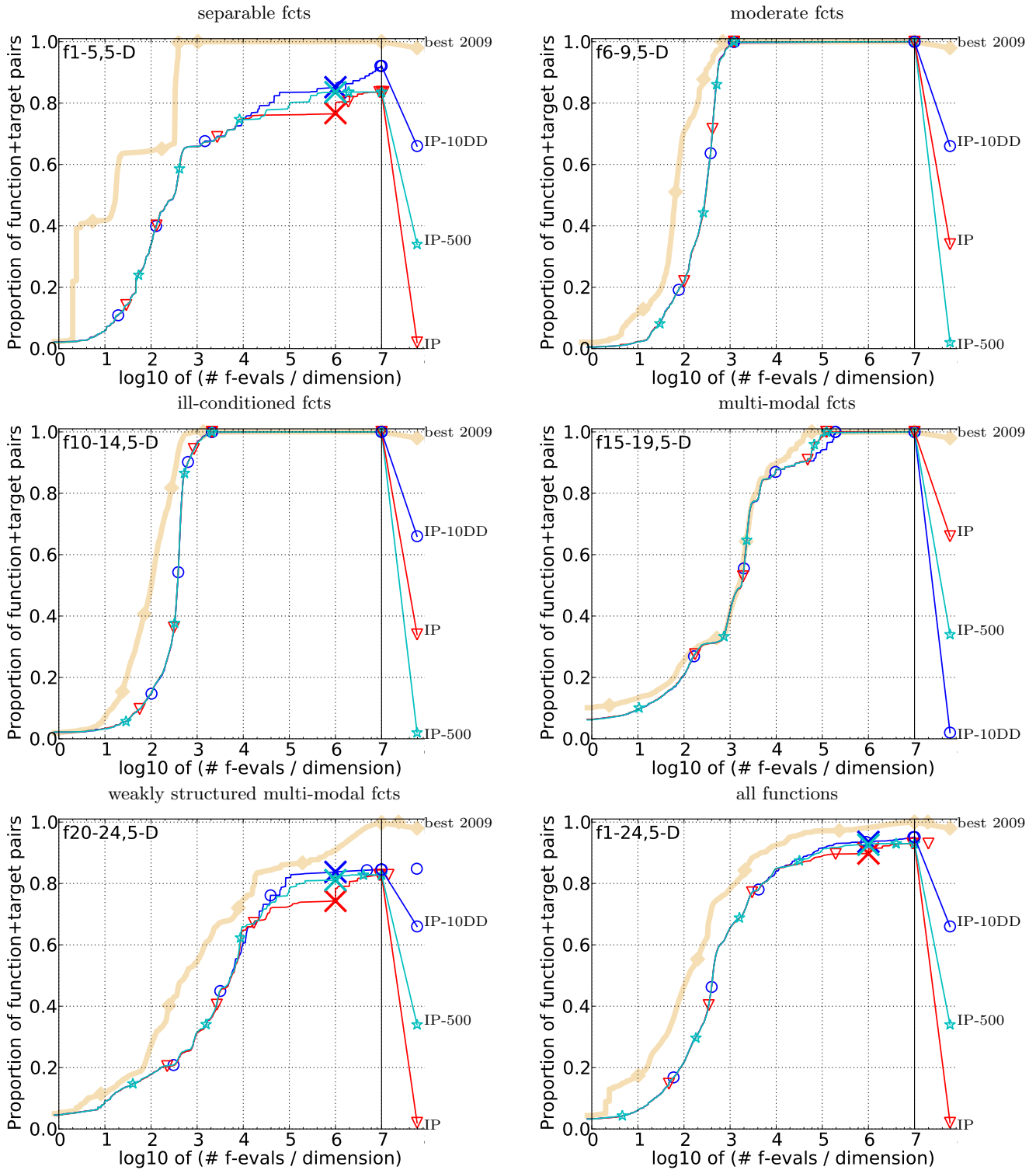


Figure 3: Bootstrapped empirical cumulative distribution of the number of objective function evaluations divided by dimension (FEvals/D) for 50 targets in $10^{[-8..2]}$ for all functions and subgroups in 5-D. The "best 2009" line corresponds to the best ERT observed during BBOB 2009 for each single target.

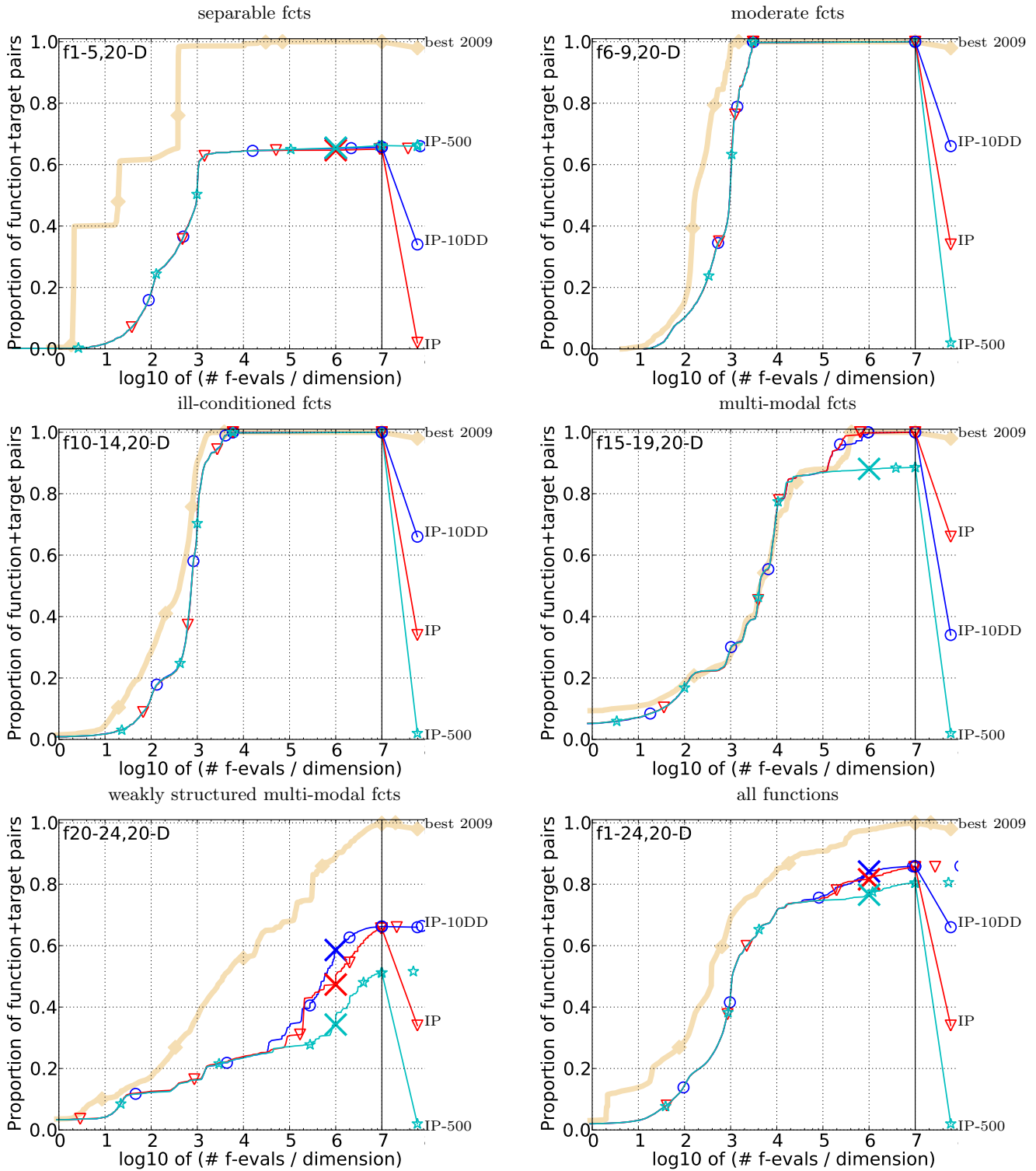


Figure 4: Bootstrapped empirical cumulative distribution of the number of objective function evaluations divided by dimension (FEvals/D) for 50 targets in $10^{[-8..2]}$ for all functions and subgroups in 20-D. The "best 2009" line corresponds to the best ERT observed during BBOB 2009 for each single target.

